Journal of Power Sources 216 (2012) 216–221

Contents lists available at SciVerse ScienceDirect

Journal of Power Sources

journal homepage: www.elsevier.com/locate/jpowsour

A lithium-ion battery separator prepared using a phase inversion process

Xiaosong Huang*

Chemical Sciences & Materials Systems Lab, GM Global R&D, 30500 Mound Rd, Warren, MI 48090, USA

HIGHLIGHTS

- Phase inversion is used to make a membrane with a uniform porous structure.
- The membrane shows satisfactory tensile strength at break.
- The membrane saturated with a liquid electrolyte enables good ionic conductance.
- Cells with this separator show excellent rate capability.

ARTICLE INFO

Article history:
Received 28 March 2012
Received in revised form
9 May 2012
Accepted 10 May 2012
Available online 28 May 2012

Keywords:
Phase inversion
Battery separator
Porous
Rate capability
Lithium ion battery

ABSTRACT

A battery separator is a porous membrane that separates the positive and negative electrodes while maintaining a good ionic flow. A method of making separators made of polyetherimide through a phase-inversion process is described. The membranes prepared by this process showed uniform porous structures as indicated by the scanning electron microscope (SEM) images. The membranes also exhibited satisfactory tensile properties and enabled high ionic conductance when saturated with a liquid electrolyte for lithium-ion batteries. Coin cells with this type of separators were prepared. Stable cycling performance and improved rate capabilities were observed when tested at room temperature.

1. Introduction

A separator is an inactive but critical component in a lithium-ion battery. It separates the positive and negative electrodes and provides the ionic conduction through the liquid electrolyte that fills in its porous structure. The most commonly used commercial separators are polyolefin separators made by either a dry process or a wet process. These polyolefin separators are mechanically strong and highly resistant to the electrolyte and electrode materials. However, they do not usually have the satisfactory dimensional stability at elevated temperatures. Conventional dry or wet process employs a stretching step to initiate and/or facilitate the formation of open porous structures. Therefore, the membranes tend to shrink at elevated temperatures due to the polymer shape memory effect increasing the risk of battery internal shorting. In addition, the separator cost remains relatively high, therefore, any reduction in separator cost will further facilitate the expansion of lithium-ion batteries in large scale applications (i.e. electric vehicles).

Phase inversion has long been used for the formation of porous structures [1–4]. It allows pore formation without stretching the structures, thus minimizing the membrane thermal shrinkage and product defects associated with the stretching step. The mass transfer of the non-solvent into the polymer solution and the solvent in the polymer solution into the non-solvent begins as soon as the cast polymer solution is exposed to a non-solvent environment. The solvent/non-solvent exchange can lead to a thermodynamically metastable and/or unstable system, thus results in the formation of a porous structure [1]. However, the mechanism has far from being fully understood. Porous polyvinylidene fluoride (PVDF) (or PVDF copolymer) [5–13] and polyacrylonitrile (PAN) (or PAN copolymer) membranes [14–18] have been fabricated through this phase inversion process and evaluated as lithium-ion battery separators. Although improved ionic conduction has been observed, the mechanical strength of these macroporous membranes needs to be improved. The United States Advanced Battery Consortium (USABC) has set its requirement on the

* Tel.: +1 586 9860836; fax: +1 586 9861207.
E-mail address: xiaosong.huang@gm.com.

0378-7753/$ – see front matter © 2012 Elsevier B.V. All rights reserved.
doi:10.1016/j.jpowsour.2012.05.019

separator tensile property as being less than 2% offset strain at 6.9 MPa (1000 psi) [19,20]. In addition, PVDF loses its mechanical strength in a liquid electrolyte, especially when the temperature is high, which may result in an increased risk of electric short when highly porous PVDF membranes are used as separators. Lithium ion battery separators made of other polymers using this phase inversion process have not been widely investigated. One of the reasons is the fact that most of the membranes prepared by the phase inversion process could not enable sufficient ionic conduction due to the existence of dense surface layers and closed porous structures.

In this work, instead of the polymers that have been used to prepare gel electrolytes, an engineering polymer, polyetherimide (PEI), was selected to form a porous structure using the phase inversion process because of its good mechanical performance and thermal stability. The membrane morphologies were adjusted through a controlled environment to achieve the improved tensile strength and uniform porous structures ensuring uniform current density distribution. A hydrophobic nano-ceramic filler was employed to open the initially closed pores in the membranes enabling a high ionic conductance without sacrificing the membrane mechanical properties evidently.

2. Materials and experiments

2.1. Chemicals and materials

Polyetherimide (PEI) was provided by Sabic Innovative Plastics (Pittsfield, MA). PEI is a high temperature polymer with excellent mechanical properties. Aerosil® R 805 (Evonic Industries, Boston, MA) was used as the nano-ceramic filler. It is a fumed silica powder that has been surface modified with an octylsilane. The treatment renders the silica extremely hydrophobic. Analytical grade N-Methyl-2-pyrrolidone (NMP) was purchased from Sigma–Aldrich (St. Louis, MO).

The cathode and anode materials used in this work were $LiNi_{1/3}Co_{1/3}Mn_{1/3}O_2$ (Toda NCM-01ST-100) (NCM) and graphite (TIMREX SLP 30), respectively. TIMREX Super P Li carbon black was used in both electrodes as the conductive additive. Kynar HSV 900 PVDF (Arkema Inc., Philadelphia, PA) was used as the binder for the electrode materials.

2.2. Experiments

PEI was dissolved in NMP at 70 °C to form a 15 wt.% solution. PEI solution and a predetermined amount of silica were then mixed to form a uniform dispersion. The dispersion was cast on a grinded glass plate by doctor's knives. The cast dispersion was either delivered into a water bath directly or conditioned in a humidity chamber of 90% R.H. and 35 °C for 20 s and then delivered into a water bath. The washing step in the water bath was used to precipitate the polymer forming a porous membrane and remove the NMP in the formed porous membrane completely. The washed membrane was then oven dried at about 110 °C for 24 h Table 1 shows how the different samples are designated. Samples 1-1, 2-1, 3-1, 4-1, and 5-1 were formed by delivering the cast dispersion into water directly and samples 1-2, 2-2, 3-2, 4-2, and 5-2 were formed by conditioning the cast dispersion in a humidity chamber of 90% R.H. and 35 °C for 20 s and then delivering it into a water bath. Membranes containing 0, 0.1, 0.2, 0.25, and 0.3 parts of silica (based on 1 part of PEI by weight) were prepared. The membrane thickness was controlled to be around 25 microns.

The dried membranes were fractured in liquid nitrogen and their fractured surfaces were examined with a scanning electron microscope (SEM).

Table 1
Designation of the membranes prepared by the phase inversion process.

Sample	Silica/PEI (by weight)	Pore formation process
1-1	0/1	Precipitation in water
1-2	0/1	Precipitation in water after conditioning at 90% R.H.
2-1	0.1/1	Precipitation in water
2-2	0.1/1	Precipitation in water after conditioning at 90% R.H.
3-1	0.2/1	Precipitation in water
3-2	0.2/1	Precipitation in water after conditioning at 90% R.H.
4-1	0.25/1	Precipitation in water
4-2	0.25/1	Precipitation in water after conditioning at 90% R.H.
5-1	0.3/1	Precipitation in water
5-2	0.3/1	Precipitation in water after conditioning at 90% R.H.

The tensile properties of the membranes were tested on Instron 5582 according to ASTM D882-09. The cross-head speed was 10 mm min^{-1}.

The membrane porosities were estimated based on the following equation:

$$P = \frac{w_T - w_s}{\rho_l \cdot V_s}$$

where w_s is the weight of the dry membrane sample, w_T is the total weight of the membrane once a liquid is fully absorbed, ρ_l is the density of the liquid, and V_s is the apparent volume of the membrane sample.

Ionic conductivity was calculated from the following equation:

$$\sigma = \frac{d}{R_b \cdot S} = \frac{1}{\rho}$$

where d is the thickness of the film, R_b is the bulk resistance, and S is the area of the electrode. Membrane samples were filled with a liquid electrolyte and sandwiched between two stainless steel electrodes. R_b was obtained using an impedance analyzer.

Battery tests such as cycle life and rate capability were carried out with a Maccor Series 4000 battery tester at 30 °C. The CR2325-type coin cells were assembled with NCM cathodes, graphite anodes, and 1 M $LiPF_6$ in ethylene carbonate (EC)/diethyl carbonate (DEC) (1:2 by volume) as the electrolyte. Cells were charged to 4.3 V under a constant-current constant-voltage mode, and then discharged to 3.0 V under a constant-current mode. For the cycle test, cells were charged at a C/5 rate and discharged at a C/5 rate in the first 5 cycles and a C/2 rate in the following cycles. For the rate capability test, cells were charged at a C/5 rate and discharged at C/5, C/2, 1C, 2C, and 4C rates. Coin cells with a commercial polypropylene separator were also tested as a baseline for comparison. The selected commercial separator was Celgard 2400, as it is a widely evaluated separator in publications. Linear sweep voltammetry was used to evaluate the membrane electrochemical stability. The membrane sample imbibed with the liquid electrolyte was sandwiched between a stainless steel electrode and a lithium foil to prepare the test cell. The cell voltage was swept at a scan rate of 1 mV s^{-1} until the onset of current flow.

3. Results and discussion

The membranes formed at different conditions showed completely different structures as indicated in Fig. 1. When the cast layer was immersed in water directly, finger-like structures with channels leading from the top to the bottom were observed as in Fig. 1 (a). It was also obvious the membrane showed a skin having a compact structure. In Fig. 1 (b) where the cast layer was conditioned at 90% R.H. first, a well-developed cellular structure was

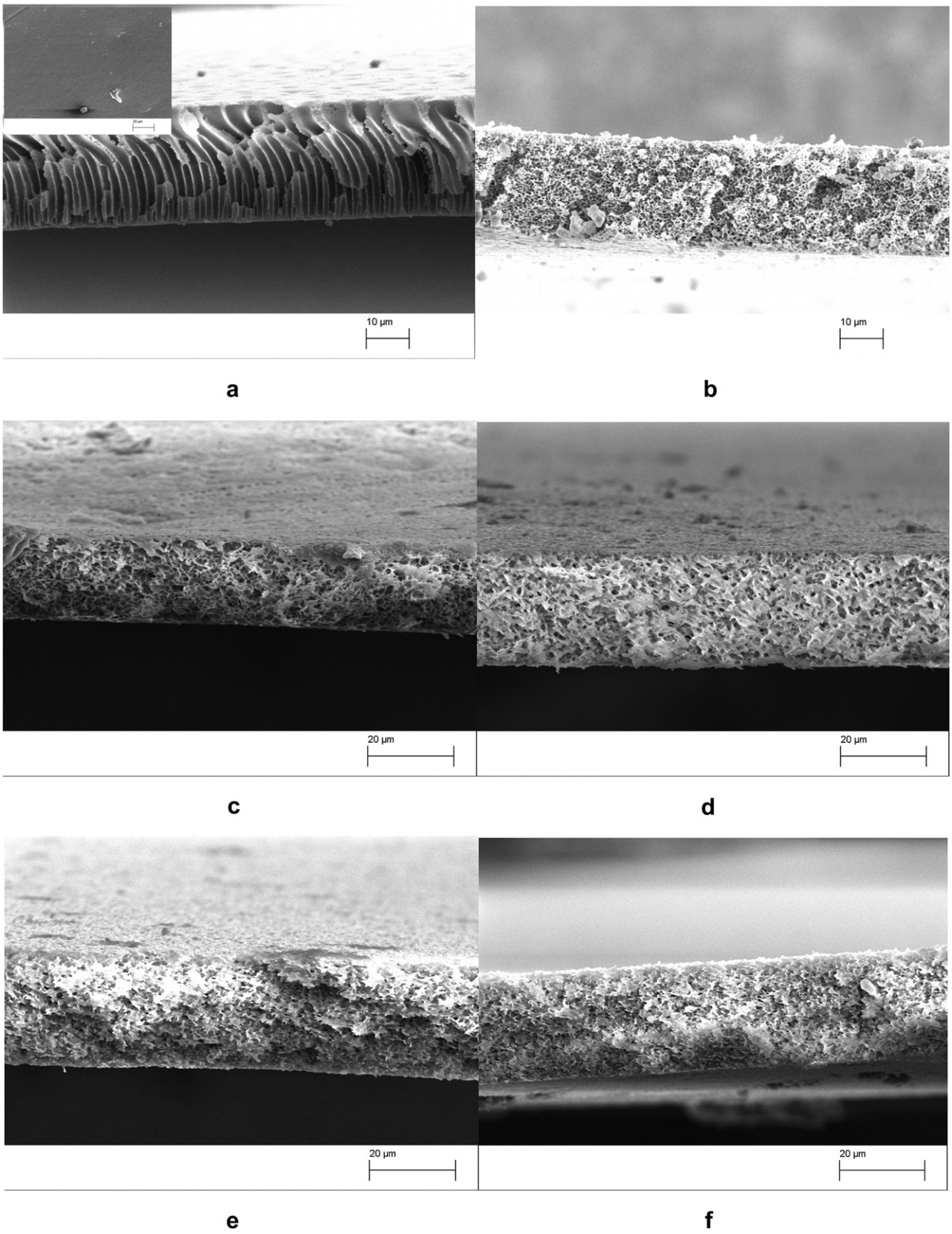

Fig. 1. SEM of the cross-section of membranes formed under different conditions. (a) 1-1, (b) 1-2, (c) 2-2, (d) 3-2, (e) 4-2 and (f) 5-2.

Table 2
Membrane porosity, ionic conductivity (after being saturated with a liquid electrolyte), and tensile strength at break.

Sample	Thickness (μm)	Porosity (%)	Ionic conductivity (mS/cm)	Tensile strength at break (MPa)
1-1	22	77	0.94	6.1±0.2
1-2	27	65	0.23	16.2±0.5
2-1	25	75	1.34	5.6±0.3
2-2	24	63	0.39	16.5±0.3
3-1	26	75	1.73	4.8±0.5
3-2	26	59	0.71	16.2±0.7
4-1	23	74	2.10	4.2±0.5
4-2	25	57	1.57	15.3±0.8
5-1	24	72	2.46	4.3±0.6
5-2	25	57	2.10	13.2±0.5
Polypropylene separator	25	~40	0.97	175.4±5.9 MPa (MD)[a] 12.6 MPa ± 2.6 (TD)[b]

[a] Machine direction.
[b] Transverse direction.

seen. The pores were uniform with the size less than 1 micron. However, the cellular structure showed no evidence of extensive interconnections. When the thin cast layer of the thermodynamically stable polymer solution is immersed in a non-solvent (water), the non-solvent/solvent/polymer mass transport takes place, which transforms the binary polymer solution into a ternary metastable/unstable solution. Phase separation is then followed forming a liquid-like polymer lean phase and a solid-like polymer rich phase. The polymer rich phase in this case is the continuous phase and the nucleation and growth of the polymer lean phase leads to the formation of porous structures. In the case where the cast layer was delivered into water directly, the formation of finger-like pores is probably caused by the very fast diffusion rates and the convection of the components. In the case where the cast layer was conditioned first, the diffusion rates are apparently slower and the concentration fluctuation and the effect of convection are very likely to be much less evident. Thus more nucleation sites are developed resulting in smaller pore sizes. Fig. 1 (c)–(f) show the SEM images where silica was added into the formulation. The addition of silica particles interconnected the cells and formed open porous structures, especially when the silica loading was higher than 0.25 parts. All these samples showed uniform porous structures. The average pore size seems to be decreased with the increase of the silica loading. The pore diameter was less than 1 micron when more than 0.25 parts of silica were added. This successfully meets the USABC requirement that the pore size should be smaller than 1 micron [19]; yet compared with the tens of nanometer-sized pores in a commercial separator, the pore diameters in these membranes are relatively big. It is valuable to investigate in further whether sub-micron pores would increase the risk of battery failure due to internal shorting, especially under abuse operating conditions.

The calculated porosities of the membranes formed under different conditions are shown in Table 2. The porosities of the membranes that were precipitated in water directly were higher than those of the membranes that were precipitated in water after humidity conditioning. It is likely that when the cast layer is conditioned, less non-solvent goes into the solution, or more solvent comes out of the solution, or both. As can be expected, the porosity decreased with increase in ceramic loading. The porosity decreased from 65% for the membrane with no silica (Membrane 1-2) to 57% for the membrane with 0.25 parts of silica (Membrane 4-2). It is worth to mention that an ideal separator should have a low porosity to allow the use of a small amount of liquid electrolytes and improve the separator mechanical properties, while still offering good ionic conductance.

Fig. 2 shows the wettability of Membrane 4-2 and the commercial separator (Celgard 2400). When a drop of liquid electrolyte (1 M $LiPF_6$ in EC/DEC (1:2 by volume)) as the electrolyte was applied, it formed a bead on the commercial separator while spread out on Membrane 4-2 in a couple of minutes, which indicates the good liquid electrolyte affinity of the PEI membrane. Polyolefin is an inherently hydrophobic polymer, thus untreated commercial separators made of polyolefin do not usually provide good electrolyte wettability. Commercial separators are normally chemically treated and/or coated with surfactants in an additional step for improved wettability.

Ionic conductivity results are also listed in Table 2. Membrane 1-1 enabled sufficient ionic conductivity due to its large pore size and high porosity. The dense skin of this membrane (also shown in the inset of Fig. 1 (a)) may have reduced the ionic conductance but the reduction was limited as the thickness of the skin was very small. Membrane 1-2 enabled a very low ionic conductivity despite its higher porosity compared to the commercial polypropylene separator. This indicates that most of the pores in this membrane were closed. The high membrane porosity is due to the existence of both

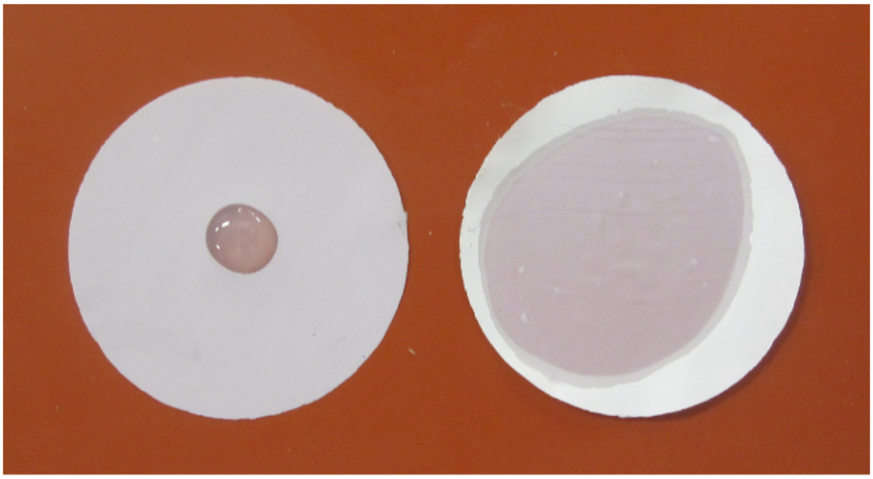

Fig. 2. Wettability by the liquid electrolyte of (a) The commercial propylene separator and (b) Membrane 4-2.

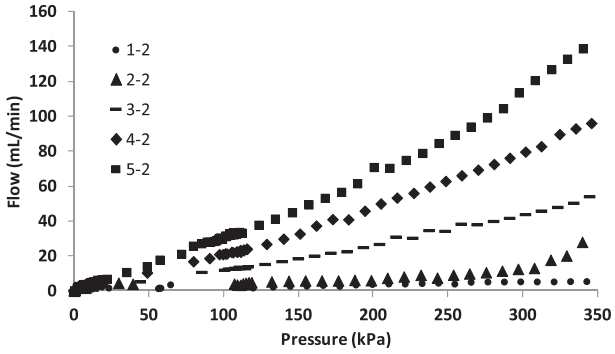

Fig. 3. Air flow rates through the membranes at different pressures.

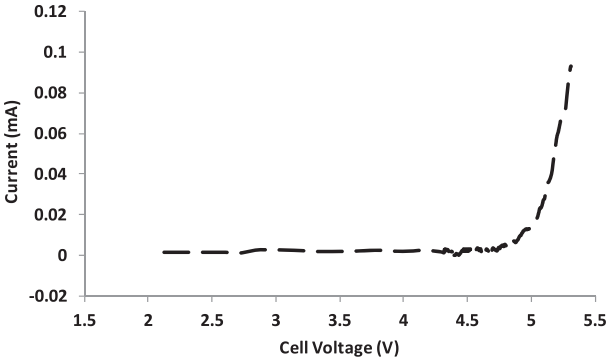

Fig. 5. Linear sweep voltammetry of membrane 4-2.

closed and open pores, but only open pores can enable ionic conductivity. Increasing the ceramic loading increased the ionic conductivity from 0.23 mS cm^{-1} to 1.57 mS cm^{-1} for the membrane with 0.25 parts of silica (Membrane 4-2) and 2.10 mS cm^{-1} for the membrane with 0.3 parts of silica (Membrane 5-2). This indicates that although the overall porosity (shown in Table 2) decreased slightly with the incorporation of silica, the open porosity may have increased. The hydrophobic silica particles penetrate the cell walls and form a weak interface with relatively hydrophilic PEI causing the formation of interconnected porous structures. Therefore, liquid electrolyte can flow through the separator to provide good ionic conduction. Alumina particles with similar particle sizes have also been investigated as fillers for PEI membranes. However, no significant improvement on the ionic conductance was observed. This interesting observation indicates that the interface between filler particles and polymer matrix may play an important role, which will need further systematic study. Compared with the 0.94 mS cm^{-1} ionic conductivity for the commercial polypropylene separator, both Membrane 4-2 and Membrane 5-2 have enabled satisfactory ionic conductivities. The good ionic conductivity when Membrane 4-2 was used as the separator can be ascribed to its better wettability by the electrolyte and its higher porosity compared to the polypropylene separator. Fig. 3 shows the air flow rates through the membranes at different pressures. It is evident that the incorporation of the silica increased the air flow rates. This observation supports the assumption that the addition of silica has led to the formation of an open porous structure.

Table 2 also shows the tensile strength of different membranes. Membrane 1-1 exhibited a low tensile strength at break of about 6 MPa. This is mainly due to the large porosity and macrovoid-like pores that extend from one surface to the other. All the membranes that have been subjected to humidity conditioning during the pore formation process showed much higher tensile strength. Increasing the ceramic loading to 0.25 parts did not decrease the tensile strength. Further increasing the ceramic loading from 0.25 parts to 0.3 parts, the tensile strength decreased from about 15.3 MPa to about 13.2 MPa. Fig. 4 is a representative stress–strain curve for membrane 4-2. It indicates the membrane has a high elongation at break of about 37% while the strain at 6.9 MPa is about 1.7%.

The electrochemical stability of Membrane 4-2 is shown in Fig. 5. The current vs. voltage curve indicates that the membrane has sufficient electrochemical stability to be cycled against the anodic potential applied in this work.

Fig. 6 shows the cell cycle performance. The *y*-axis indicates the capacity retention ratio calculated by dividing the discharge capacity of the nth cycle by the discharge capacity of the first cycle. At 30 °C, the graphite/NCM cell with a 4-2 separator showed stable cyclability in the tested 50 cycles. The capacity retention ratios of the cells with the 4-2 separator and a commercial polypropylene separator were respectively about 86% and 81% at the end of the first 50 cycles. The higher capacity retention ratio for the cell with the 4-2 separator is likely due to the higher inter-electrode (electrolyte + separator) ionic conduction enabled by the new separator.

Fig. 7 presents the rate capabilities of the cells with different separators. For both the cells with a 4-2 separator and the commercial untreated polypropylene separator, the discharge capacities decreased gradually with the increase in C rate, which reflects the polarization. Cells with both separators showed similar capacity retention ratios at low discharge rates, i.e. C/5, C/2, and 1C rates. However, at 2C and 4C discharge rates, it is evident that the cell with the 4-2 separator shows higher capacity retention ratios than the cell with the conventional polypropylene separator. The capacity retention ratios of the cell with Membrane 4-2 were about

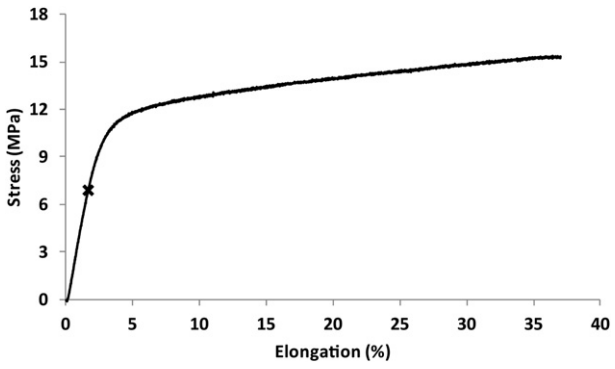

Fig. 4. A representative stress–strain curve for membrane 4-2.

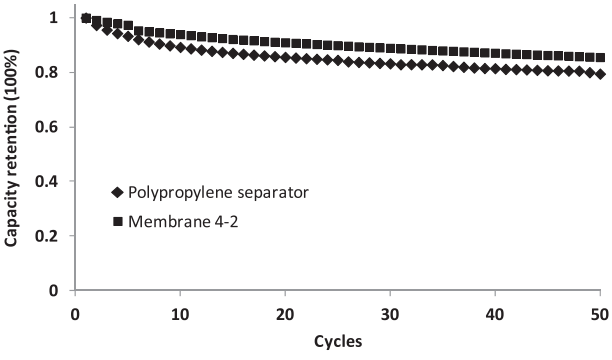

Fig. 6. Cycle performance of the coin cells with the commercial separator and membrane 4-2.

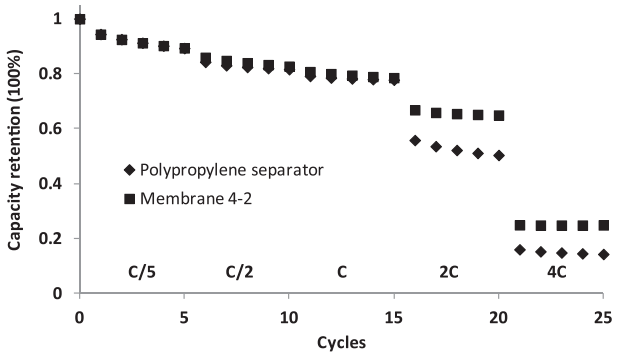

Fig. 7. Rate capability of the coin cells with the commercial separator and membrane 4-2.

66% at 2C and 25% at 4C, while they were respectively about 54% and 15% for the cell with the polypropylene separator. The good rate performance is an indication of a low internal polarization, which is confirmed by the conductivity test results in Table 2 as Membrane 4-2 enabled a high ionic conductivity.

4. Conclusions

A phase inversion approach was successfully used to prepare porous membranes for battery separator applications. The membranes showed uniform porous structures with an average pore size less than 1 micron. The membrane with 0.25 parts of nano-silica (based on 1 part of polymer) showed satisfactory tensile strength at break of about 15.3 MPa. The ionic conductivity of this membrane when saturated with a liquid electrolyte was about 1.57 mS cm^{-1}. Separator performance was also evaluated by testing CR2325-type graphite/NCM coin cells. Cells with this membrane as the separator showed stable cycling performance and improved rate capability. The capacity retention ratio of the cell with this membrane as the separator was about 66% at a 2C discharge rate, while it was about 54% for the cell with a conventional polypropylene separator.

Acknowledgments

The author would like to thank Dr. Yan Wu for helpful discussions and providing electrode materials. The author would also like to thank Drs. Ion Halalay and Yar-Ming Wang for the assistance with the conductivity tests.

References

[1] C. Stropnik, L. Germic, B. Zerjal, J. Appl. Polym. Sci. 61 (1996) 1821–1830.
[2] C. Stropnik, V. Kaiser, Desalination 145 (2002) 1–10.
[3] H. Strathmann, K. Kock, Desalination 3 (1977) 241–255.
[4] P. vandeWitte, P.J. Dijkstra, J.W.A. vandenBerg, J. Feijen, J. Membr. Sci. 117 (1996) 1–31.
[5] F. Boudin, X. Andrieu, C. Jehoulet, I.I. Olsen, J. Power Sources 81 (1999) 804–807.
[6] A. Magistris, E. Quartarone, P. Mustarelli, Y. Saito, H. Kataoka, Solid State Ionics 152 (2002) 347–354.
[7] A. Du Pasquier, P.C. Warren, D. Culver, A.S. Gozdz, G.G. Amatucci, J.M. Tarascon, Solid State Ionics 135 (2000) 249–257.
[8] Q. Shi, W. Huang, X. Zhou, Y.S. Yan, C.R. Wan, Acta Polym. Sin 134 (2004) 350–354.
[9] Z.H. Li, G.Y. Su, X.Y. Wang, D.S. Gao, Solid State Ionics 176 (2005) 1903–1908.
[10] K.M. Kim, N.G. Park, K.S. Ryu, S.H. Chang, Electrochim. Acta 51 (2006) 5636–5644.
[11] Q. Shi, M.X. Yu, X. Zhou, Y.S. Yan, C.R. Wan, J. Power Sources 103 (2002) 286–292.
[12] J.H. Cao, B.K. Zhu, Y.Y. Xu, J. Membr. Sci. 281 (2006) 446–453.
[13] Z.H. Li, P. Zhang, H.P. Zhang, Y.P. Wu, X.D. Zhou, Electrochem. Commun. 10 (2008) 791–794.
[14] H.S. Min, D.W. Kang, D.Y. Lee, D.W. Kim, J. Polym. Sci. Pol. Phys. 40 (2002) 1496–1502.
[15] S.S. Zhang, M.H. Ervin, K. Xu, T.R. Jow, Electrochim. Acta 49 (2004) 3339–3345.
[16] Z. Tian, X.M. He, W.H. Pu, C.R. Wan, C.Y. Jiang, Electrochim. Acta 52 (2006) 688–693.
[17] G. Wu, H.Y. Yang, H.Z. Chen, F. Yuan, L.G. Yang, M. Wang, R.J. Fu, Mater. Chem. Phys. 104 (2007) 284–287.
[18] Q.Z. Xiao, X.Z. Wang, W. Li, Z.H. Li, T.J. Zhang, H.L. Zhang, J. Membr. Sci. 334 (2009) 117–122.
[19] X. Huang, J. Solid State Electr. 15 (2011) 649–662.
[20] P. Arora, Z. Zhang, Battery Separators, Chem. Rev. 104 (2004) 4419–4462.